

**Are your MRI contrast agents cost-effective?**

Learn more about generic Gadolinium-Based Contrast Agents.



**AJNR**

**Whole-Brain DTI Assessment of White Matter Damage in Children with Bilateral Cerebral Palsy: Evidence of Involvement beyond the Primary Target of the Anoxic Insult**

This information is current as of April 8, 2024.

F. Arrigoni, D. Peruzzo, C. Gagliardi, C. Maghini, P. Colombo, F. Servodio Iammarrone, C. Pierpaoli, F. Triulzi and A.C. Turconi

*AJNR Am J Neuroradiol* published online 17 March 2016  
<http://www.ajnr.org/content/early/2016/03/17/ajnr.A4717>

# Whole-Brain DTI Assessment of White Matter Damage in Children with Bilateral Cerebral Palsy: Evidence of Involvement beyond the Primary Target of the Anoxic Insult

 F. Arrigoni,  D. Peruzzo,  C. Gagliardi,  C. Maghini,  P. Colombo,  F. Servodio Iammarrone,  C. Pierpaoli,  F. Triulzi, and  A.C. Turconi



## ABSTRACT

**BACKGROUND AND PURPOSE:** Cerebral palsy is frequently associated with both motor and nonmotor symptoms. DTI can characterize the damage at the level of motor tracts but provides less consistent results in nonmotor areas. We used a standardized pipeline of analysis to describe and quantify the pattern of DTI white matter abnormalities of the whole brain in a group of children with chronic bilateral cerebral palsy and periventricular leukomalacia. We also explored potential correlations between DTI and clinical scale metrics.

**MATERIALS AND METHODS:** Twenty-five patients (mean age, 11.8 years) and 25 healthy children (mean age, 11.8 years) were studied at 3T with a 2-mm isotropic DTI sequence. Differences between patients and controls were assessed both voxelwise and in ROIs obtained from an existing DTI atlas. Clinical metrics included the Gross Motor Function Classification System, the Manual Ability Classification System, and intelligence quotient.

**RESULTS:** The voxel-level and ROI-level analyses demonstrated highly significant ( $P < .001$ ) modifications of DTI measurements in patients at several levels: cerebellar peduncles, corticospinal tracts and posterior thalamic radiations, posterior corpus callosum, external capsule, anterior thalamic radiation, superior longitudinal fasciculi and corona radiata, optic nerves, and chiasm. The reduction of fractional anisotropy values in significant tracts was between 8% and 30%. Statistically significant correlations were found between motor impairment and fractional anisotropy in corticospinal tracts and commissural and associative tracts of the supratentorial brain.

**CONCLUSIONS:** We demonstrated the involvement of several motor and nonmotor areas in the chronic damage associated with periventricular leukomalacia and showed new correlations between motor skills and DTI metrics.

**ABBREVIATIONS:** AD = axial diffusivity; CP = cerebral palsy; CST = corticospinal tract; FA = fractional anisotropy; GMFCS = Gross Motor Function Classification System; HC = healthy control; IQ = intelligence quotient; MACS = Manual Ability Classification System; MD = mean diffusivity; PVL = periventricular leukomalacia; RD = radial diffusivity; SCP = superior cerebellar peduncle

Cerebral palsy (CP) is one of the leading causes of disabilities in children in Western countries, affecting 1–2.5 per 1000 live births.<sup>1</sup> The term CP includes a heterogeneous spectrum of non-

progressive brain disorders manifesting with motor, sensory, and cognitive deficits.<sup>2</sup> Even if motor impairment often represents the most remarkable manifestation of the disorder, disturbances of sensation, perception, cognition, communication, and behavior commonly affect patients' quality of life.

Conventional MR imaging helps determine the gross brain pathology associated with CP: Periventricular leukomalacia (PVL) is the most common pattern of injury demonstrated by MR imaging in preterm children (low birth weight or very low birth weight) with CP.<sup>3</sup> PVL is characterized by a dilation of the lateral ventricles, in particular at the level of the occipital horns, reduction of WM volume, hyperintense signal of the residual periventricular WM on T2-weighted and FLAIR images, and thinning of the corpus callosum. These findings reflect the loss of neuronal cells and gliosis demonstrated by pathology.<sup>3</sup>

More recently, diffusion-weighted MR imaging and DTI have been used to understand the microstructural changes occurring in the brains of patients with CP both in the acute and chronic


Received October 12, 2015; accepted after revision January 5, 2016.

From the Neuroimaging Lab (F.A., D.P.), Functional Neurorehabilitation Unit (C.G., C.M., F.S.I., A.C.T.), and Child Psychopathology Unit (P.C.), Scientific Institute IRCCS Eugenio Medea, Bosisio Parini, Italy; National Institutes of Health (C.P.), Bethesda, Maryland; and Department of Neuroradiology (F.T.), Fondazione IRCCS Ca' Granda, Ospedale Maggiore Policlinico, Milano, Italy.


This work was supported by the Italian Ministry of Health (Ricerca Corrente 2012 to A.C. Turconi).

Paper previously presented as an electronic poster at: Annual Meeting of the European Society of Neuroradiology, September 17–20, 2015; Naples, Italy.

Please address correspondence to Filippo Arrigoni, MD, Scientific Institute IRCCS Eugenio Medea, Via don L. Monza 20, 23842, Bosisio Parini (Lecco), Italy; e-mail: filippo.arrigoni@bp.inf.it

 Indicates open access to non-subscribers at [www.ajnr.org](http://www.ajnr.org)

 Indicates article with supplemental on-line appendix and tables.

 Indicates article with supplemental on-line photos.

<http://dx.doi.org/10.3174/ajnr.A4717>

phases. Quantitative measurements derived from DTI,<sup>4</sup> mostly fractional anisotropy (FA) and mean diffusivity (MD), have been successfully used to demonstrate structural modifications of the corticospinal tract (CST) and ascending sensorimotor tracts (including the posterior thalamic radiations) of patients with CP.<sup>5</sup> However, a quantification of the impairment of different tracts measured by DTI is lacking. Most studies<sup>5</sup> focus on reporting the significant differences between patients and controls but not on the magnitude of the differences, which could instead provide valuable information about the severity of damage to each tract. More detailed descriptions of the characteristics and amount of the damage could contribute to a more precise clinical definition and could help in targeting more specific rehabilitation interventions, thus improving their efficacy.

Moreover, despite the presence of important nonmotor symptoms, the evidence of the involvement of cerebral commissures and association tracts and of the frontal, temporal, and occipital lobes is not consistent.<sup>5</sup> Data on corpus callosum and association tracts such as the superior and inferior longitudinal fasciculi are conflicting, with some studies showing FA reductions in patients with CP<sup>6,7</sup> and others showing no differences compared with controls.<sup>8–10</sup>

Given these premises, in this article, we applied a standardized pipeline of analysis of DTI data to a group of children with PVL and bilateral CP to do the following:

- 1) Assess the pattern of WM abnormalities in the whole brain, extending beyond motor areas.
- 2) Quantify the severity of the alterations in terms of FA modifications to detect the most affected tracts.
- 3) Correlate diffusion metrics with cognitive and clinical features.

## MATERIALS AND METHODS

The study took place at Scientific Institute IRCCS Eugenio Medea. This study was approved by the local ethics committee, and written informed parental consent was obtained for all participants.

### Patients

Twenty-five children (16 males, mean age,  $11.8 \pm 3.1$  years; age range, 7.7–16.8 years; 20 right-handed) with a diagnosis of spastic bilateral CP were included in the study. Children were selected from the clinical database of the Functional Neurorehabilitation Unit of Eugenio Medea Institute and underwent a clinical and radiologic protocol developed as part of a research study on CP. Subject selection criteria were the following:

- Preterm birth (<37 weeks of gestation).
- Diagnosis of spastic bilateral CP with a known history of anoxic or hypoxic injuries associated with labor and delivery.
- PVL as described on the MR imaging report of previous examinations.
- Age older than 7 years to perform MR imaging without sedation.
- Visual Acuity more than three-tenths (Snellen Letter Acuity Test), corresponding to normal or mildly reduced visual acuity, not consistent with a severe visual impairment.

**Table 1: Demographic and clinical characteristics of patients with CP and HCs**

	Patients with Bilateral CP	Healthy Controls	Statistics	
Participants (No.)	25	25		
Sex (M/F)	16:09	17:08	$\chi^2 = 0.62$	$P < .43$
Age at MRI (yr)	$11.8 \pm 3.1$	$11.8 \pm 2.8$	$t = 0.027$	$P > .97$
Gestational age (wk)	$31.8 \pm 3.1$	$38.8 \pm 1.3$	$U = 197$	$P < .001$
IQ	$68.8 \pm 19.6$	$121 \pm 18.7$	$U = 18.5$	$P < .001$
MACS (I, II, III)	9, 10, 6	—		
GMFCS (I, 2, 3, 4)	9, 4, 8, 4	—		

- Mild-to-moderate gross motor and upper limb functional impairment.

The recruited participants were classified according to the Classification of Cerebral Palsy and the Surveillance of Cerebral Palsy in Europe algorithms. Their motor function was assessed according to the Gross Motor Function Classification System (GMFCS),<sup>11</sup> while handling of objects in daily activities was classified according to the Manual Ability Classification System (MACS).<sup>12</sup> General intelligence abilities were assessed by the age-appropriate Wechsler Scale.<sup>13</sup>

Twenty-five healthy controls (HCs) (8 females; mean age,  $11.8 \pm 2.8$  years; age range, 7.6–16.8 years; 20 right-handed) with no history of psychiatric or neurologic illness, learning disabilities, or hearing or visual loss were recruited to be matched with patients with CP. HCs showed average school performances in language, and reading and had an intelligence quotient (IQ) of at least 85 on the Cattell's Culture Fair Intelligence Test, a nonverbal culture-free test to measure the analytic and reasoning ability in abstract and novel situations with a fair correlation index with the IQ in the Wechsler Scales.<sup>14</sup>

Emotional and behavioral problems were assessed by the Child Behavioral Checklist and Youth Self Report.<sup>15</sup> None of the healthy subjects exceeded the clinical cutoff ( $T = 63$ ) in the Total Problems Scale.

Demographic details of the entire group are shown in Table 1.

### MR Imaging and DTI Protocol

All the examinations were performed on the same 3T scanner (Achieva; Philips Healthcare, Best, the Netherlands) equipped with a 32-channel head coil and included both conventional MR imaging and DTI sequences.

Conventional MR imaging included a 3D T1-weighted sequence ( $TR = 8.2$  ms,  $TE = 3.8$  ms, flip angle =  $8^\circ$ ,  $FOV = 210 \times 210$  mm<sup>2</sup>, acquired matrix =  $210 \times 210 \times 170$ , voxel size =  $1 \times 1 \times 1$  mm) and a 2D T2-weighted turbo spin-echo sequence with a high in-plane resolution on the axial plane ( $TR = 4100$  ms,  $TE = 82$  ms, flip angle =  $90^\circ$ ,  $FOV = 230 \times 230$  mm, acquired matrix =  $550 \times 420$ , section thickness = 3 mm, reconstructed voxel size =  $0.22 \times 0.22 \times 3$  mm).

DTI data were acquired with the same sequence in all subjects. We used a multishell 2D T2-weighted EPI sequence ( $TR = 8645$  ms,  $TE = 63$  ms, flip angle =  $90^\circ$ ,  $FOV = 224 \times 224$  mm<sup>2</sup>, acquired matrix =  $112 \times 112$ , section thickness = 2 mm, final voxel size =  $2 \times 2 \times 2$  mm<sup>3</sup>), including 15 directions at  $b = 300$  s/mm<sup>2</sup>, 53 directions at  $b = 1100$  s/mm<sup>2</sup>, and 8 volumes at  $b = 0$

s/mm<sup>2</sup> (see the On-line Appendix for a detailed explanation of the DTI acquisition scheme).

Moreover, a T2-weighted structural volume was acquired with a fat-suppressed TSE sequence to correct DTI data for susceptibility-induced EPI distortion artifacts as described by Wu et al<sup>16</sup> (TR = 3000 ms, TE = 100 ms, FOV = 224 × 224 mm<sup>2</sup>, acquired matrix = 112 × 112, section thickness = 1.7 mm, voxel size = 2 × 2 × 1.7 mm).

### **Morphologic Damage**

T1- and T2-weighted images of each patient were reviewed by the same experienced neuroradiologist (F.A., with 8 years of experience in pediatric neuroradiology), blinded to clinical data, to confirm the presence of PVL diagnosed in previous examinations and to assess and quantify, on a visual scale, the severity of the cerebral damage. To assess the homogeneity of our cohort in terms of WM damage, 3 parameters were taken into account: ventricular dilation, WM involvement (thinning and hyperintense abnormal signal on T2-weighted images), and corpus callosum thinning. Each structure was visually classified as mildly, moderately, or severely involved according to its appearance on morphologic sequences. A global assessment of WM damage was obtained combining the appearance of the 3 structures (the overall damage was considered moderate or severe if at least 2 or 1 structure, respectively, was moderately or severely involved; otherwise the pattern of injury was considered mild) (On-line Fig 1). Brain injury at the level of gray matter structures such as the basal ganglia and thalami was evaluated separately.

### **DTI Processing**

DTI processing was performed by using the TORTOISE software (<http://tortoisedi.nichd.nih.gov/stbb/login.html>).<sup>17</sup> The preprocessing pipeline included a motion-correction step, a correction of image distortions (eg, eddy current, B0 susceptibility, EPI distortion) by using the nondistorted T2-weighted volume as a reference,<sup>16,18</sup> a realignment to the anterior/posterior commissure plane, and an upsampling to a final voxel resolution of 1.5 × 1.5 × 1.5 mm.

Data were then visually inspected to detect remaining artifacts and/or wrong preprocessing results. Corrupted volumes were discarded from the subsequent analysis.

The DTI tensor was computed by using the nonlinear least squares method described by Chang et al,<sup>19</sup> and FA, MD, axial diffusivity (AD), and radial diffusivity (RD) maps were then calculated for each subject.

A study DTI template was built from all subject tensors (patients and controls) with the DTI-ToolKit software package (<http://software.incf.org/software/dti-toolkit-dti-tk>),<sup>20</sup> which uses a spatial registration algorithm based on the diffusion tensor similarity to achieve a better alignment of WM structures. All subject tensors were moved to the template space performing only 1 interpolation operation, and scalar diffusion maps were subsequently derived in the template space for the voxel-level statistical analysis.

ROIs for the ROI-level analysis were derived from the Johns Hopkins atlases of WM included in FSL (<http://www.fmrib.ox.ac.uk/fsl>). More precisely, the 20 ROIs representing the most important WM tracts of the brain included in the Johns Hopkins

University WM tractography atlas<sup>21,22</sup> were integrated with ROIs derived from the ICBM-DTI-81 atlas ([http://www.loni.usc.edu/atlas/Atlas\\_Detail.php?atlas\\_id=15](http://www.loni.usc.edu/atlas/Atlas_Detail.php?atlas_id=15)),<sup>23</sup> to obtain an extensive coverage of both the supra- and infratentorial WM. The warp field between the Johns Hopkins University template and the DTI study template was computed and combined with the subject-DTI study template warp field to move the ROIs from the Johns Hopkins University template to the single subject space. For each ROI, the mean FA, MD, AD, and RD values were computed for the statistical analysis.

### **Statistical Analysis**

Differences in clinical measures between the HC and the CP groups were investigated with the  $\chi^2$  for sex, the *t* test for age at MR imaging, and the Mann-Whitney test for gestational age and IQ.

For all DTI comparisons, significance was set at  $P \leq .001$  (corrected for multiple comparisons), to be very conservative and detect the most relevant differences between groups. Statistical analysis at the voxel level was performed by using the permutation test implemented by Winkler et al,<sup>24</sup> with the threshold-free cluster enhancement method. Statistical analysis at the ROI level was performed by using Matlab (MathWorks, Natick, Massachusetts), and the significance threshold was set to  $P < .001$ , corrected for multiple comparisons (false discovery rate).

The General Linear Model was used to model the data both at the voxel and ROI levels by using age as the predictor. Moreover, the Pearson correlation coefficients between the diffusion values and the clinical variables (GMFCS, MACS, IQ) were computed.

## **RESULTS**

### **Descriptive Results and Clinical Features**

All participants (HCs and patients with CP) completed the study protocol (MR imaging and clinical evaluations). HCs and patients with CP differed in gestational age and IQ, but not for mean age at MR imaging and sex distribution (Table 1). Gross motor function, manipulation, and general cognitive ability scales showed a large range of values in the CP group. Considering gross motor functions, mild or moderate impairment (class I and II at GMFCS) was present in 13 patients (52%), while severe impairment (class IV at GMFCS) was present only in 4 (16%). As to handling and manipulation abilities measured by MACS, mild impairment (MACS I and II) was noted in 19 patients (76%), while no patients had severe impairment (MACS IV). Full IQ ranged from 38 to 109, with a mean of  $68.8 \pm 19.6$  (Table 1). Mild cognitive impairment (IQ = 50–70) was noted in 9 children (36%), moderate cognitive impairment (IQ < 50) was noted in 4 children (16%), whereas 12 children (48%) had no cognitive impairment (IQ > 70). Mean gestational age at birth was  $31.8 \pm 3.1$  weeks, ranging from 27 to 37 weeks.

No correlation was found between the level of impairment by MACS and GMFCS and IQ score or gestational age, but GMFCS scores were correlated to MACS scores ( $r = 0.82$ ).

### **Pattern of Damage at Conventional MR Imaging**

The results of the classification of cerebral WM damage based on the visual inspection of T1- and T2-weighted imaging is reported



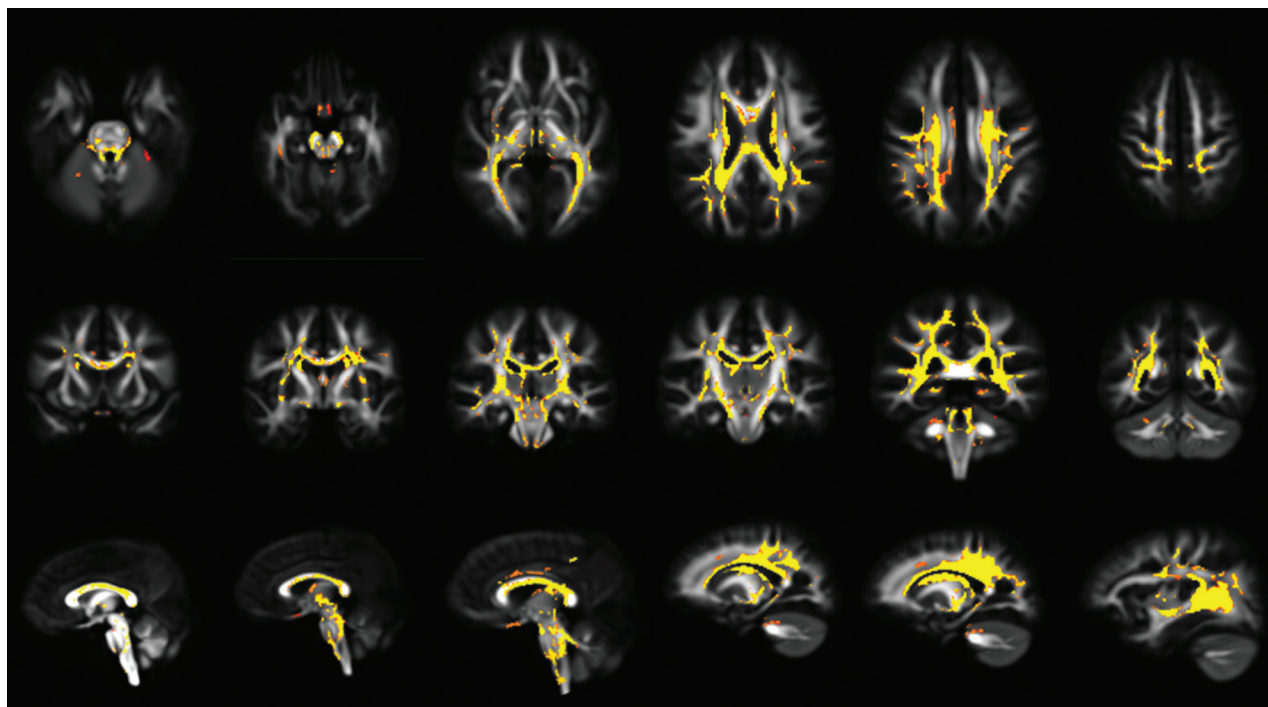


**FIG 1.** Axial (first row), coronal (second row), and sagittal (third row) MR images show voxelwise FA group differences between patients with CP and HCs (FA patients < FA controls). Results are overlaid on the FA template obtained from all subjects, at a significance level of  $P < .001$ , corrected for multiple comparisons.

in On-line Table 1. In 16/25 cases (64%), the severity of PVL was mild, and it was moderate in 7 (28%). Severe WM damage was found in only 2 patients (8%). Thalamic or basal ganglia atrophy was found in 8 cases (32%).

Voxel-based DTI results for the whole-brain voxel-based analysis demonstrated significant differences ( $P < .001$ ) of FA values between patients with CP and HCs: Visual group comparison detected a diffuse reduction of FA values in both the supratentorial and infratentorial WM (Fig 1). The areas affected were bilaterally located in the superior and inferior cerebellar peduncles (including decussation), motor and sensory tracts in the brain stem, posterior limbs of internal capsules, peritrigonal WM (including the optic and thalamic radiations), external capsules, centrum semiovale, corpus callosum (with a prevalent involvement of its central portion), fornix, cingulum, chiasm, and optic tracts. The same regions in the supratentorial WM showed increased MD, AD, and RD values at the same significance level ( $P < .001$ ) (On-line Fig 2). No significant differences were detected for MD, AD, and RD in the brain stem and cerebellum, except for an RD increase at the level of cerebellar and cerebral peduncles (On-line Fig 2). No regions in the brain showed increased FA or decreased MD, AD, and RD in patients with CP compared with controls.

#### ROI-Level DTI Results

In On-line Table 2, we show mean FA values in the 43 tracts derived from the DTI atlas for both patients with CP and HCs. Mean MD, AD, and RD values are reported in On-line Table 3. When we set a conservative threshold of  $P < .001$ , differences in FA and other DTI metrics emerged in motor areas (like CSTs and thalamic radiations), but also in nonmotor pathways such as the middle and posterior parts of the corpus callosum, optic radia-

tions, superior longitudinal fasciculi, cingulum, and cerebellar peduncles.

The magnitude of the differences of FA mean values for significant tracts ( $P < .001$ ) is reported in Fig 2, where percentage differences of patients with CP versus HCs ( $\Delta$ FA) and corresponding  $z$  scores are also shown. The magnitude of the differences varied among tracts. In patients with CP, posterior corona radiata, thalamic radiations, corpus callosum, cingulum, and superior cerebellar peduncles showed a large FA reduction, between 15% and 30%. Other significant tracts showed a less pronounced FA reduction, between 8% and 15%.

On-line Tables 4 and 5 summarize the correlations between the level of impairment of motor skills (by GMFCS and MACS) and DTI measures. With a significance threshold of .001, no correlations emerged, while some correlations were significant when the threshold was set at  $< .05$ . In particular, FA values in the corticospinal tracts, posterior thalamic radiations, corona radiata, and superior longitudinal fasciculus showed significant negative correlations with both GMFCS and MACS. FA mean values of the inferior cerebellar peduncle, inferior fronto-occipital fasciculus, inferior longitudinal fasciculus, and uncinate fasciculus were negatively correlated with GMFCS, but not with MACS. Few tracts showed positive correlations between other DTI measures (MD, AD, RD) and GMFCS or MACS.

No significant correlations were found between IQ score and DTI measures in the ROIs at both  $P < .05$  and  $< .001$ .

#### DISCUSSION

In this study, we assessed abnormal findings on diffusion MR imaging associated with PVL in preterm children affected by bi-

## FA differences

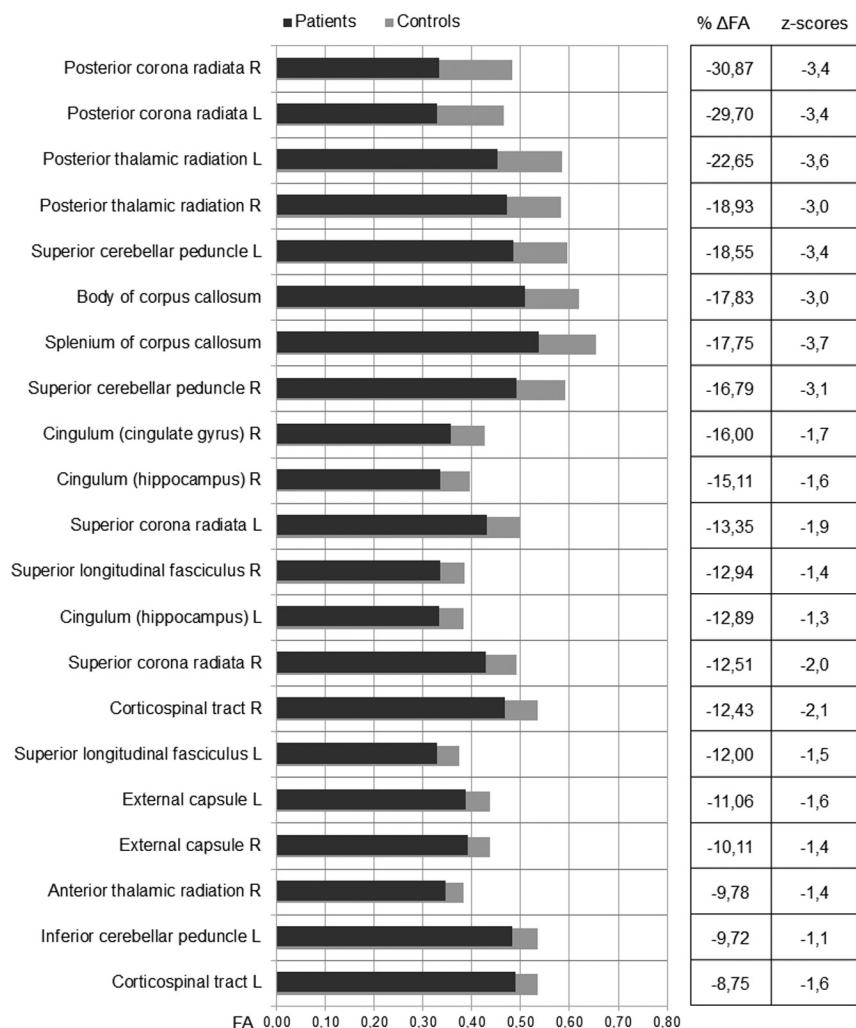


**FIG 2.** The bar graph shows the mean FA values for patients with CP and HC in tracts that showed significant ( $P < .001$ ) differences. Tracts are listed according to the percentage differences ( $\Delta FA$ ) between patients with CP and HCs, reported in the right column. Z scores for each tract are also shown. R indicates right; L, left.

lateral cerebral palsy. Through both a voxel-level and an atlas-based ROI approach, we extended our investigation beyond the analysis of corticospinal and sensory-motor tracts that were extensively investigated in previous studies.<sup>8,25-30</sup> Our analysis took into account, with a standardized and non-operator-dependent method, a large number of WM tracts and areas extensively covering both the supratentorial and infratentorial brain and the cerebellum.

Moreover, we did not limit our observations to significance maps and averaged values, but we also examined the magnitude of the differences of DTI measures between patients with CP and HCs and correlated these data with clinical cognitive and motor indices.

We focused on WM organization and damage, both in motor and nonmotor areas. We hypothesized that the alteration of cerebral organization and connections in CP could involve multiple tracts and areas, thus mirroring the complex clinical features.

Recent literature<sup>8,25-30</sup> has extensively documented, through

DTI, the damage occurring to corticospinal and sensory-motor tracts in patients with CP. Less attention has been paid to the severity of the alterations and to the different degrees of involvement that can affect WM tracts.

The distribution of WM abnormalities measured by DTI confirmed, in our patients with PVL, a prevalent involvement of CSTs, the posterior part of corpus callosum, posterior corona radiata, and thalamic radiations, with a less severe involvement of anterior brain regions.

These findings indicate that the atlas-based ROI approach we used provided results consistent with the non-atlas-based methods that have been used in previous studies.<sup>7,31</sup> Moreover, we extended our observation to the severity of DTI modifications, discovering that FA was less reduced in CSTs (8.75%, 12.43%) than in the posterior thalamic radiations (approximately 20%); thus, these findings testified to the well-known importance of sensory integration in the determinism of the multilevel damage in CP. The FA difference between HCs and participants with CP was also quite relevant (approximately 17%) in the cerebellar peduncles and corpus callosum. The involvement of cerebellar peduncles could be the result of a secondary degeneration due to WM damage. These alterations can contribute to the motor impairment observed in patients with CP, given that cerebrocerebellar connections between the cerebellum and thalami through the superior cerebellar peduncles (SCPs) are necessary for motor functions.<sup>32</sup> The same mechanisms may be valid for the corpus callosum, whose integrity is fundamental for coordination and movement, but also for cognition.

Therefore, as we observed, even in patients with milder forms of bilateral spastic CP and PVL, the impairment of the descending pyramidal fibers could be a relatively minor feature, whereas the damage of other parts of the neuronal network involved in motor control (such as the corpus callosum and cerebellum) may have a larger impact.<sup>6</sup>

Moreover, as we showed, the complex PVL damage affects many projections and associative tracts far beyond those involved in motor planning and control, thus contributing to the complex clinical pattern that characterizes bilateral CP.<sup>5,32,33</sup> We found a severe involvement of optic tracts, optic radiations, and posterior corona radiata that could affect the integrity of the afferent sensory visual tracts with much more evidence than previously described.<sup>32,34</sup> Although our recruitment criteria excluded children

with major visual problems, visual perceptual difficulties characterize the cognitive profile in children with PVL<sup>35</sup> and can be linked to damage to the visual afferent pathways and visual processing. The diffuse damage in the anteroposterior associative and commissural tracts may explain the impairment in problem solving and executive functions.

Different from Wang et al,<sup>32</sup> we failed to find a correlation between mean FA values in WM tracts and cognitive competences. This failure could be explained by the different ages of the 2 cohorts: Wang et al studied very young children, with a mean age of 16 months, while we studied older patients (mean age, 11.8 years). Brain maturation and growth could affect WM structures and DTI measures and explain the different correlations found, as recently demonstrated in the meta-analysis by Li et al.<sup>36</sup> Also the different methodology used in cognitive assessment (developmental quotient versus IQ) may have played a role.

This study has limitations. First, the parenchymal damage in subjects with CP, with loss of WM volume and ventricular enlargement, may influence the creation of a common DTI template between patients and HCs and affect DTI results. However, our cohort showed only mild ventricular enlargement in 68% of patients, and the effects of the distortions applied by the transformation used to build the template and the results of single-subject registrations were carefully inspected and corrected to prevent possible errors.

Second, the use of noncontinuous scales such as the GMFCS and MACS for correlations with WM damage is suboptimal; however, this method has been used in previous studies in patients with CP.<sup>32</sup>

## CONCLUSIONS

Our study demonstrates that the structural WM damage affecting children with CP affects not only structures that are the primary target of the anoxic insult in the preterm, such as thalamic radiations and periventricular WM, but it also strongly affects other distant tracts and pathways like the SCPs, optic nerves and tracts, and long associative fasciculi. These elements can help to better understand the pattern of clinical impairment in CP and can be a prerequisite for the developing targeted rehabilitation-training programs that could improve the performance of such patients. In particular, the magnitude of tract injury, as measured by DTI metrics, may be used in the future as a biomarker for monitoring the effect of cognitive and motor rehabilitative programs.

Disclosures: Filippo Arrigoni—RELATED: Grant: Ministero della Salute (RC 2012);\* UNRELATED: Grants/Grants Pending: Ministero della Salute (RC 2013);\* Chiara Gagliardi, Cristina Maghini, Anna Carla Turconi—RELATED: Grant: Ministero della Salute-Italia (RC 2012);\* Money paid to the institution.

## REFERENCES

- Reid SM, Carlin JB, Reddihough DS. Rates of cerebral palsy in Victoria, Australia, 1970 to 2004: has there been a change? *Dev Med Child Neurol* 2011;53:907–12 CrossRef Medline
- Rosenbaum P, Paneth N, Leviton A, et al. A report: the definition and classification of cerebral palsy April 2006. *Dev Med Child Neurol Suppl* 2007;109:8–14 Medline
- Volpe JJ. Brain injury in premature infants: a complex amalgam of destructive and developmental disturbances. *Lancet Neurol* 2009;8:110–24 CrossRef Medline
- Basser PJ, Pierpaoli C. Microstructural and physiological features of tissues elucidated by quantitative-diffusion-tensor MRI. *J Magn Reson B* 1996;111:209–19 CrossRef Medline
- Scheck SM, Boyd RN, Rose SE. New insights into the pathology of white matter tracts in cerebral palsy from diffusion magnetic resonance imaging: a systematic review. *Dev Med Child Neurol* 2012;54:684–96 CrossRef Medline
- Koerte I, Pelavin P, Kirmess B, et al. Anisotropy of transcallosal motor fibres indicates functional impairment in children with periventricular leukomalacia. *Dev Med Child Neurol* 2011;53:179–86 CrossRef Medline
- Yoshida S, Hayakawa K, Yamamoto A, et al. Quantitative diffusion tensor tractography of the motor and sensory tract in children with cerebral palsy. *Dev Med Child Neurol* 2010;52:935–40 CrossRef Medline
- Murakami A, Morimoto M, Yamada K, et al. Fiber-tracking techniques can predict the degree of neurologic impairment for periventricular leukomalacia. *Pediatrics* 2008;122:500–06 CrossRef Medline
- Thomas B, Eyssen M, Peeters R, et al. Quantitative diffusion tensor imaging in cerebral palsy due to periventricular white matter injury. *Brain* 2005;128:2562–77 CrossRef Medline
- Nagae LM, Hoon AH Jr, Stashinko E, et al. Diffusion tensor imaging in children with periventricular leukomalacia: variability of injuries to white matter tracts. *AJNR Am J Neuroradiol* 2007;28:1213–22 CrossRef Medline
- Palisano RJ, Rosenbaum P, Bartlett D, et al. Content validity of the expanded and revised Gross Motor Function Classification System. *Dev Med Child Neurol* 2008;50:744–50 CrossRef Medline
- Eliasson AC, Krumlinde-Sundholm L, Rösblad B, et al. The Manual Ability Classification System (MACS) for children with cerebral palsy: scale development and evidence of validity and reliability. *Dev Med Child Neurol* 2006;48:549–54 CrossRef Medline
- Wechsler D. *Manual for the Wechsler Intelligence Scale for Children-Revised*. New York: Psychological Corporation; 1974
- Cattell R. *Culture Free Intelligence Test, Scale 2, Handbook*. Champaign: Institute of Personality and Ability Testing; 1949
- Achenbach TM, Rescorla LA. *Manual for the ASEBA School-Age Forms and Profiles*. Burlington: University of Vermont, Research Center for Children, Youth, and Families; 2001
- Wu M, Chang LC, Walker L, et al. Comparison of EPI distortion correction methods in diffusion tensor MRI using a novel framework. *Med Image Comput Comput Assist Interv* 2008;11:321–29 Medline
- Pierpaoli C, Walker L, Irfanoglu MO, et al. TORTOISE: an integrated software package for processing of diffusion MRI data. In: *Proceedings of the International Society for Magnetic Resonance in Medicine*, Stockholm, Sweden; May 1–7, 2010: 1597
- Rohde GK, Barnett AS, Basser PJ, et al. Comprehensive approach for correction of motion and distortion in diffusion-weighted MRI. *Magn Reson Med* 2004;51:103–14 CrossRef Medline
- Chang LC, Jones DK, Pierpaoli C. RESTORE: robust estimation of tensors by outlier rejection. *Magn Reson Med* 2005;53:1088–95 CrossRef Medline
- Zhang H, Yushkevich PA, Rueckert D, et al. Unbiased white matter atlas construction using diffusion tensor images. *Med Image Comput Comput Assist Interv* 2007;10:211–18 Medline
- Wakana S, Caprihan A, Panzenboeck MM, et al. Reproducibility of quantitative tractography methods applied to cerebral white matter. *Neuroimage* 2007;36:630–44 CrossRef Medline
- Hua K, Zhang J, Wakana S, et al. Tract probability maps in stereotaxic spaces: analyses of white matter anatomy and tract-specific quantification. *Neuroimage* 2008;39:336–47 CrossRef Medline
- Mori S, Oishi K, Jiang H, et al. Stereotaxic white matter atlas based on diffusion tensor imaging in an ICBM template. *Neuroimage* 2008;40:570–82 CrossRef Medline
- Winkler AM, Ridgway GR, Webster MA, et al. Permutation infer-

- ence for the general linear model. *Neuroimage* 2014;92:381–97 CrossRef Medline
25. Bleyenheuft Y, Grandin CB, Cosnard G, et al. Corticospinal dysgenesis and upper-limb deficits in congenital hemiplegia: a diffusion tensor imaging study. *Pediatrics* 2007;120:e1502–11 CrossRef Medline
  26. Glenn OA, Ludeman NA, Berman JI, et al. Diffusion tensor MR imaging tractography of the pyramidal tracts correlates with clinical motor function in children with congenital hemiparesis. *AJNR Am J Neuroradiol* 2007;28:1796–802 CrossRef Medline
  27. Trivedi R, Agarwal S, Shah V, et al. Correlation of quantitative sensorimotor tractography with clinical grade of cerebral palsy. *Neuroradiology* 2010;52:759–65 CrossRef Medline
  28. Chang MC, Jang SH, Yoe SS, et al. Diffusion tensor imaging demonstrated radiologic differences between diplegic and quadriplegic cerebral palsy. *Neurosci Lett* 2012;512:53–58 CrossRef Medline
  29. Cho HK, Jang SH, Lee E, et al. Diffusion tensor imaging-demonstrated differences between hemiplegic and diplegic cerebral palsy with symmetric periventricular leukomalacia. *AJNR Am J Neuroradiol* 2013;34:650–54 CrossRef Medline
  30. Lennartsson F, Holmström L, Eliasson AC, et al. Advanced fiber tracking in early acquired brain injury causing cerebral palsy. *AJNR Am J Neuroradiol* 2015;36:181–87 CrossRef Medline
  31. Rha DW, Chang WH, Kim J, et al. Comparing quantitative tractography metrics of motor and sensory pathways in children with periventricular leukomalacia and different levels of gross motor function. *Neuroradiology* 2012;54:615–21 CrossRef Medline
  32. Wang S, Fan G, Xu K, et al. Potential of diffusion tensor MR imaging in the assessment of cognitive impairments in children with periventricular leukomalacia born preterm. *Eur J Radiol* 2013;82:158–64 CrossRef Medline
  33. Yoshida S, Faria AV, Oishi K, et al. Anatomical characterization of athetotic and spastic cerebral palsy using an atlas-based analysis. *J Magn Reson Imaging* 2013;38:288–98 CrossRef Medline
  34. Lee JD, Park HJ, Park ES, et al. Motor pathway injury in patients with periventricular leukomalacia and spastic diplegia. *Brain* 2011;134:1199–210 CrossRef Medline
  35. Melhem ER, Hoon AH Jr, Ferrucci JT Jr, et al. Periventricular leukomalacia: relationship between lateral ventricular volume on brain MR images and severity of cognitive and motor impairment. *Radiology* 2000;214:199–204 CrossRef Medline
  36. Li K, Sun Z, Han Y, et al. Fractional anisotropy alterations in individuals born preterm: a diffusion tensor imaging meta-analysis. *Dev Med Child Neurol* 2015;57:328–38 CrossRef Medline